



## Dynamic behavior of the viscosity and density in the Belousov-Zhabotinsky reaction

Minoru Yoshimoto<sup>1\*</sup>, Shingo Kubo<sup>1</sup>, Masanao Hirose<sup>1</sup>, Shohta Masuda<sup>1</sup>, Shigeru Kurosawa<sup>2</sup>

<sup>1</sup>Department of Bioengineering, Faculty of Engineering, Kagoshima University, 1-21-40 Korimoto, Kagoshima 890-0065, (JAPAN)

<sup>2</sup>National Institute of Advanced Industrial Science and Technology (AIST), 1-1 Higashi, Tsukuba 305-8565, (JAPAN)

Received: 21<sup>st</sup> September, 2007 ; Accepted: 26<sup>th</sup> September, 2007

### ABSTRACT

We investigated the dynamic behavior between the redox potential and the solution viscosity and density of the BZ reaction by the systematic variation of the mixing level of the solution and the solution viscosity and density. The mixing level was controlled by the stirrer bar speed, and the solution viscosity and density was changed by the addition of the Polyoxyethylen (10) octylphenyl Ether (Triton X-100). This study has revealed that the three types of the oscillations with the phase difference appear depending on the mixing level and the solution viscosity and density of the BZ reaction. It has also become clear that the critical micellization concentration (cmc) play an important role in the behavior of the oscillation of the solution viscosity and density.

© 2007 Trade Science Inc. - INDIA

### KEYWORDS

Belousov-Zhabotinsky reaction;  
QCM;  
viscosity and density.

### INTRODUCTION

The Belousov-Zhabotinsky (BZ) reaction is well-known as one of the most famous oscillating chemical reactions. The BZ reaction exhibits a wide variety of nonlinear phenomena, e.g., target pattern or spiral pattern in an unstirred shallow solution, and multistability, periodicity, multiperiodicity or deterministic chaos in a stirred solution<sup>[1-3]</sup>.

The chemical wave in the unstirred shallow solution of the BZ reaction has features that differ significantly from the familiar reaction-diffusion wave, because the convective mass transport plays a relevant role. The effects of the convection on the propagation of the

chemical wave have been observed experimentally<sup>[4-6]</sup>. The convection enhances the chemical wave speed and affects the curvature of the front. The natural convection disturbs a traveling wave and the disturbed wave affects a convection pattern. This hydrodynamic effect is strongly affected by the solution viscosity and density. Recently, it has been reported that, in the unstirred batch system, the solution viscosity and density of the BZ reaction behaved as a bifurcation parameter for the sequence chaos → quasi-periodicity → period-1 and, in the stirred batch system, affected the oscillation period and the duration of the rising portion of the oscillatory cycle<sup>[7-9]</sup>. It is obvious that the solution viscosity and density of the BZ reaction plays an important role

in the spatial and the temporal patterns.

On the other hand, the mixing effects on the BZ reaction have been reported<sup>[10-12]</sup>. These effects include the include changes in both the frequency and the amplitude of the oscillation, and quenching of spontaneous oscillations. The mixing also plays an important role in the BZ reaction.

In the previous studies, the oscillation of the BZ reaction has been monitored only by the change of the redox potential and the absorbance. On the other hand, in our recent paper<sup>[13]</sup>, we have reported that the quartz crystal microbalance (QCM) was able to directly measure the dynamic behavior of the solution viscosity and density of the BZ reaction  $\sqrt{\rho_L \eta_L}$  ( $\eta_L$  and  $\rho_L$  are the absolute viscosity and the density of a solution, respectively)<sup>[14,15]</sup>. However, the dynamic behavior between the redox potential and the solution viscosity and density of the BZ reaction is not still revealed in detail. Therefore, in this paper, we investigate its dynamic behavior by the systematic variation of the mixing level and the solution viscosity and density. Especially, we focus our aim on the phase difference between the redox potential and the solution viscosity and density.

## EXPERIMENTAL

Malonic acid,  $\text{NaBrO}_3$ ,  $\text{H}_2\text{SO}_4$ ,  $\text{FeSO}_4 \cdot 7\text{H}_2\text{O}$ ,  $\text{KBr}$  (WAKO Pure Chemical Industries, Ltd., Japan) and O-Phenanthroline- $\text{H}_2\text{O}$  (DOJINDO, Japan) were of commercial analytical grade and were used without further purification. The solution of  $[\text{Fe}(\text{Phen})_3]^{2+}$ , ferroin, was prepared by dissolving  $\text{FeSO}_4 \cdot 7\text{H}_2\text{O}$  and O-Phenanthroline- $\text{H}_2\text{O}$  in the pure water with the specific resistance of 18.2 Mohm·cm. The water was purified by the Milli-Q apparatus (Millipore, Japan) and was deaerated before the experiments. In the present experiments, we employed the system of  $[\text{malonic acid}] = 0.29\text{M}$ ,  $[\text{NaBrO}_3] = 0.28\text{M}$ ,  $[\text{ferroin}] = 0.69\text{mM}$ ,  $[\text{H}_2\text{SO}_4] = 0.57\text{M}$  and  $[\text{KBr}] = 0.067\text{M}$ .

The schematic diagram of the experimental setup is illustrated in figure 1a. The BZ reaction was performed using 30ml solution in the batch reactor (31 mm in diameter and 46 mm in depth). The batch reactor was covered with the water jacket. The temperatures were kept at  $25 \pm 0.1^\circ\text{C}$ . The redox potential of the BZ

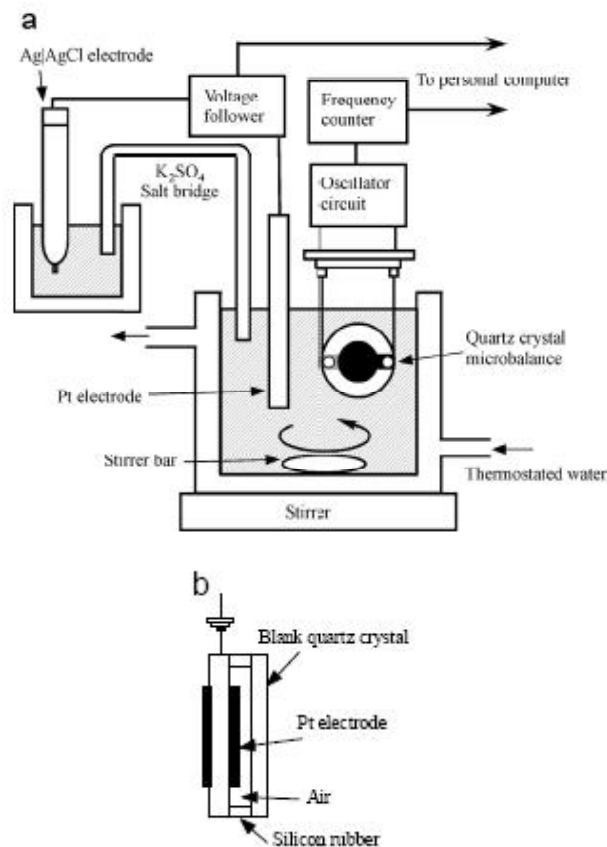


**Figure 1 :** (a) Schematic illustration of the experimental setup. The Pt and Ag | AgCl electrodes, and the quartz crystal microbalance (QCM) were used to measure the redox potential and the solution viscosity and density ( $\sqrt{\rho_L \eta_L}$ ) of the BZ reaction, respectively. (b) Schematic diagram of the one-face sealed QCM.

reaction ( $\Delta E$ ) was measured between the platinum electrode and the Ag|AgCl electrode (HORIBA 2060A-10T, Japan), using the  $\text{K}_2\text{SO}_4$  salt bridge. The Pt and Ag | AgCl electrodes were connected to the IBM-compatible PC through the voltage follower.

In general, the viscosity and the density of the solution change at the same time. In case of the BZ reaction, the resonant-frequency shift of the QCM ( $\Delta F$ ) is mainly generated by the viscous penetration depth generated on the oscillating QCM, that is,  $\sqrt{\rho_L \eta_L}$ <sup>[11,12]</sup>. In order to monitor  $\sqrt{\rho_L \eta_L}$  of the BZ reaction, the 9MHz AT-cut QCM (SEIKO EG & G, Ltd., Japan) was employed. The QCM had the configuration of the round of 8 mm diameter and a pair of the round platinum electrodes of 5mm diameter (Figure 1b). The QCM was

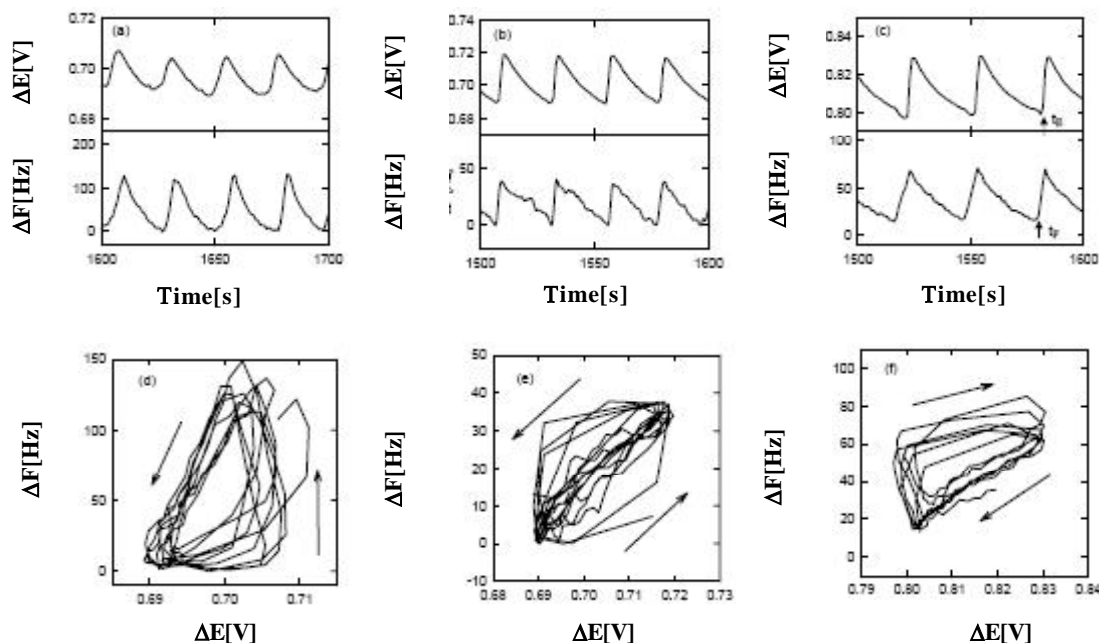


**Figure 2 :** Time series and phase portraits of the BZ reaction. (a), (b) and (c) are the time series of  $\Delta E$  and  $\Delta F$ . (d), (e) and (f) are the phase portraits composed from the time series of (a), (b) and (c), respectively. (a) and (d): the oscillation phase of the redox potential is advanced for that of  $\Delta F$  (the stirrer bar speed is 50 rpm and the concentration of Triton-X is 0.020 wt%). (b) and (e): the oscillation phases of both the redox potential and the  $\Delta F$  are almost equal (150 rpm and 0.010 wt%). (c) and (f): the oscillation phase of  $\Delta F$  is advanced for that of the redox potential (500 rpm and 0.010 wt%). The arrows in the phase portraits indicate the direction of movement

connected into a series resonant TTL circuit (SEIKO EG&G QCA917-21, Japan), which caused the QCM to oscillate at the resonant frequency near 9MHz. The TTL circuit was powered from a 5V dc supply. The resonant-frequency shift was monitored by the universal frequency counter (Agilent technologies 53131A) connected to the PC measuring the redox potential. The sampling times of both the redox potential and the resonant frequency were set at 0.1 s.

In the present experiments, the one side of the QCM was sealed with a blank quartz crystal casing (Figure 1b), maintaining it in an air environment, while the other side was contacted with the solution of the BZ reaction. This casing is essential for the frequency stability of the QCM in an ionic solution<sup>[16]</sup>. The one-face sealed QCM was vertically immersed into the solution of the BZ reaction (Figure 1a).

The mixing levels of the solution of the BZ reaction were controlled using the stirrer bar (20mm in length and 5mm in diameter) and the magnetic stirrer (AS ONE ML-101, Japan). The solution viscosity and density of the BZ reaction was varied using the Polyoxyethylene

(10) octylphenyl Ether (Triton X-100) (WAKO Pure Chemical Industries, Ltd., Japan), which was added in preparation of the solution of the BZ reaction.

## RESULTS AND DISCUSSION

In order to investigate in detail the dynamic behavior between the redox potential and the solution viscosity and density, we systematically varied the stirrer bar speed and the solution viscosity and density. Figure 2 shows the time series of  $\Delta E$  and  $\Delta F$ , and the  $\Delta E$ - $\Delta F$  phase portraits. It is obvious that  $\Delta F$  changes in a rhythmic manner, synchronized with the oscillation of  $\Delta E$ : when  $\Delta E$  is high (the ratio of the Fe(III) complex to Fe(II) complex is high),  $\Delta F$  is high. We have found that the typical three types of the oscillations with the phase difference appear depending on the stirrer speed and the solution viscosity and density. That is,  
 Type-I: The oscillation phase of  $\Delta E$  is advanced for that of  $\Delta F$  (Figures 2(a) and 2(d)),  
 Type-II: The oscillation phase of both  $\Delta E$  and  $\Delta F$  is the same (Figures 2(b) and 2(e)),

Type-III: The oscillation phase of  $\Delta F$  is advanced for that of  $\Delta E$  (Figures 2(c) and 2(f)).

In these cases, when the phase difference time ( $\tau$ ) is  $-1s \leq \tau \leq +1s$ , the phases of both are the same, when  $\tau < -1s$ , the oscillation phase of  $\Delta E$  is advanced and when  $\tau > +1s$ , the oscillation phase of  $\Delta F$  is advanced, where  $\tau = t_E - t_F$  ( $t_E$  and  $t_F$  are the times of the rising points of the oscillations of  $\Delta E$  and  $\Delta F$ , respectively, see figure 2c). Here, we employ the average values calculated from 10 oscillations.

Generally, when the QCM is dipped into a solution, its resonant-frequency shift depends on  $\sqrt{\rho_L \eta_L}$ . The relationship between the resonant-frequency shift of the one-face sealed QCM and  $\sqrt{\rho_L \eta_L}$  is described by the following equation<sup>[14]</sup>:

$$\Delta f = -\frac{f_0^2}{\sqrt{\pi \rho \mu}} \sqrt{\rho_L \eta_L} \quad (1)$$

where  $\Delta f$  is the resonant-frequency shift due to a solution viscosity,  $f_0$  the resonant fundamental frequency of a quartz crystal,  $\mu$  the shear modulus of a quartz crystal and  $\rho$  the densities of a quartz crystal. Equation 1 quantitatively explains the relationship between the resonant-frequency shift and the viscosity and density of a Newtonian liquid. From figure 2, the average amplitudes of  $\Delta F$  of (a), (b) and (c) are 109, 40 and 57 Hz, respectively. Here, using eq 1, we attempted to convert  $\Delta F$  into the concentration of the sucrose at 20°C, where the sucrose solution is known as the Newtonian liquid. This attempt revealed that  $\Delta F = 109, 40$  and  $57$  Hz corresponded to about 4, 1.5 and 2 wt%, respectively. The average periods of  $\Delta F$  of (a), (b) and (c) are 24, 24 and 30s, respectively. On the other hand, the average amplitudes of  $\Delta E$  of (a), (b) and (c) are 15.5, 29.7 and 31.6 mV, respectively, and the average periods of  $\Delta E$  are approximately the same as those of  $\Delta F$ .

In the present paper, we are especially interested in the dynamic behavior of the phase difference between  $\Delta E$  and  $\Delta F$  of the BZ reaction. To investigate it, we systematically changed the stirrer bar speed and the solution viscosity and density. The results are indicated in figure 3. Figure 3 illustrates the region of the three types of the oscillation with the phase difference. Region-I means the region of the Type-I oscillation. The

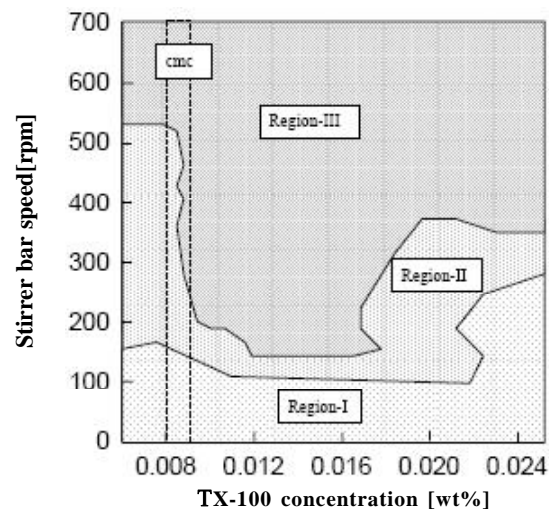


**Figure 3 :** Diagram of the phase difference between  $\Delta E$  and  $\Delta F$  of the BZ reaction. Region-I shows the region of the Type-I oscillation. Region-II shows the region of the Type-II oscillation. Region-III shows the region of the Type-III. The region between two dashed lines (0.008~0.009 wt%) shows the critical micellization concentration (cmc). The diagram is constructed from the average values calculated from 10 oscillations

Type-I oscillation appears in the low speed of the stirrer bar over the present Triton X-100 concentration. On the other hand, the Type-III oscillation appears in Region-III. This area is wide and occupies the part of the high speed of the stirrer bar over the present Triton X-100 concentration. The Type-II oscillation is generated in the region between Region-I and Region-III. These results show that when the mixing level of the solution is low, the Type-I oscillation is dominant, and that when the mixing is high, the Type-III oscillation is lying above those for the other two types.

In the previous paper, we have proposed that the solution viscosity and density may be dependent on the degree of the decrease of the catalyst electrostriction and the number of the water molecules rearranged due to the variation of the electric charge of the catalyst. The oscillations of the Type-I and the Type-III oscillations are described by the above explanation. However, in the Type-III oscillation, the oscillation phase of  $\Delta F$  comes before that of  $\Delta E$ . It seems that this phenomenon is inconsistent with the previous description. However, the behavior of  $\Delta E$  and  $\Delta F$  in the critical micellization concentration (cmc) may give a clue. In figure 3, the cmc region is shown, where the cmc was

## Full Paper

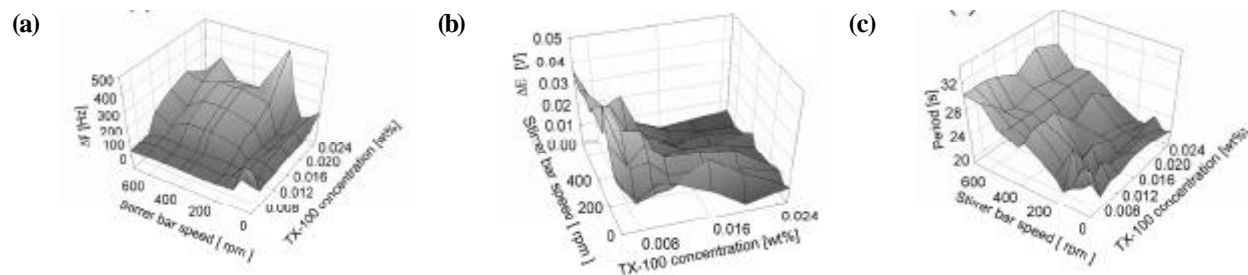


**Figure 4:** Three-dimensional graphs of the variation of the amplitudes and the periods of  $\Delta E$  and  $\Delta F$ . (a) the variation of the amplitude of  $\Delta F$  against stirrer bar speed and the Triton X-100 concentration. (b) the variation of the amplitude of  $\Delta E$  against stirrer bar speed and the Triton X-100 concentration. (c) the variation of periods of oscillations. We employ the average values calculated from 10 oscillations

measured using the QCM. The boundary line between Region-II and Region-III changes drastically within the region of the cmc. On the other hand, the boundary line between Region-I and Region-II changes slightly. This phenomenon suggests that the cmc may play an important role in the oscillation of the solution viscosity and density. The micelle is formed above the cmc. This micelle accelerates the Type-III oscillation by the interaction with the catalyst. The platinum electrode and the QCM measure the redox potential and the solution viscosity and density at the macro level, respectively. On the other hand, the previous explanation discusses its phenomenon at the molecular level. That is, the propagation speed from the molecular level to the macro level is very important in the measurement of the macro level of the redox potential and the solution viscosity and density. Above the cmc or in the high mixing level, the propagation speed of the solution viscosity and density is advanced for that of the redox potential. On the other hand, in the low mixing level, the propagation speed of the redox potential is advanced, because, in the low mixing level, the interactions between the catalyst, the micelle and the water become weak. Above 0.022wt% of the Triton X-100, the boundary line of Region-I increases again. This phenomenon indicates that the mixing effects may be weakened by the increase of the solution viscosity and the propagation speed of the solution viscosity and density from the molecular level to the macro level may be retarded in that of the redox potential. To gain the further insight into the mechanism of the behavior of the phase difference between  $\Delta E$  and  $\Delta F$ , we are now studying.

Figure 4 shows the variation of the amplitudes of

$\Delta E$  and  $\Delta F$  and the oscillation period against the stirrer bar speed and the Triton X-100 concentration. The amplitudes of  $\Delta F$  increase above the cmc and above 150 rpm of the stirrer bar speed (Figure 4a). It is obvious that the cmc and the stirrer bar speed affect the oscillation of the solution viscosity and density. In addition, the amplitudes of  $\Delta F$  increase again above 0.022wt% and in 150~200rpm. These results support the above explanation of the three types of oscillations. On the other hand, in all stirrer bar speeds, the amplitudes of  $\Delta E$  decrease with an increase in the Triton X-100 concentration (Figure 4b). This phenomenon is the same as that reported by Paul.<sup>9</sup> The hydrodynamic characters of the surfactant affect the amplitudes of  $\Delta E$ . The oscillation periods increase with stirrer bar speed in all Triton X-100 concentrations (Figure 4c). The tendency of this phenomenon is the same as that described by Menzinger and Jankowski<sup>[11]</sup>. This phenomenon is generated by the homogenous intervention of the reactive gases.

In the present paper, we have systematically investigated the dynamic behavior between the redox potential and the viscosity and density of the BZ reaction solution. This study has revealed that the three types of the oscillations with the phase difference appear depending on the stirrer bar speed and the solution viscosity and density. We have also found that the region of the existence of the Type-III oscillation is wide and appears in the high mixing levels, i.e., homogenous solution. The variation of the solution viscosity and density may be important in the organisms. The cells of the organisms have constantly the inflow and outflow of ions. The inflow and outflow of ions cause the variation

of the intracellular quantity of the electric charge. Naturally, this phenomenon accompanies with the variation of the solution viscosity and density within the cells. This change of the viscosity and density of the intracellular solution may affect the DNA control within the cells.

**REFERENCES**

- [1] B.P.Belousov; Sb.Ref.Radiats.Med., **1**, 145 (1959).
- [2] A.N.Zaikin, A.N.Zhabotinsky; Nature, London, **225**, 535 (1970).
- [3] S.K.Scott; 'Chemical Chaos', 1<sup>st</sup> ed. Oxford University Press, Oxford, (1991).
- [4] G.Bazsa, I.R.Epstein; J.Phys.Chem., **89**, 3050 (1985).
- [5] H.Miike, S.C.Müller, B.Hess; Chem.Phys.Lett., **144**, 515 (1988).
- [6] J.A.Pojman, I.R.Epstein; J.Phys.Chem., **94**, 4966 (1990).
- [7] N.Marchettini, M.Rustici; Chem.Phys.Lett., **317**, 647 (2000).
- [8] M.Rustici, R.Lombardo, M.Mangone, C.Sbriziolo, V.Zambrano, M.L.Turco Liveri; Faraday Discuss., **120**, 39 (2001).
- [9] A.Paul; J.Phys.Chem.B, **109**, 9639 (2005).
- [10] Y.Luo, I.R.Epstein; J.Chem.Phys., **85**, 5733 (1986).
- [11] M.Menzinger, P.Jankowski; J.Phys.Chem., **90**, 1217 (1986).
- [12] F.Ali, M.Menzinger; J.Phys.Chem., **95**, 6408 (1991).
- [13] M.Yoshimoto, H.Shirahama, S.Kurosawa, M.Naito; J.Chem.Phys., **120**, 7067 (2004).
- [14] K.K.Kanazawa, J.G.Gordoni; Anal.Chim.Acta, **175**, 99 (1985).
- [15] D.A.Buttry, M.D.Ward; Chem.Rev., **92**, 1355 (1992).
- [16] F.Caruso, H.Rinia, D.N.Furlong; J.Colloid Interface Sci., **178**, 104 (1996).